Proceedings for: the Interplay between Local and Global Processes in Galaxies
Cozumel, México, 11th-15th April, 2016

Connecting Small and Large Scales: The Role of Feedback in Establishing Global Galaxy Properties over Cosmic Times

Rhea-Silvia Remus[1] & Klaus Dolag[1,2]

[1]Universitäts-Sternwarte München, LMU München, Scheinerstr. 1, D-81679 München, Germany
[2]Max-Planck-Institute for Astrophysics, Karl-Schwarzschild-Str. 1, D-85741 Garching, Germany
e-mail: rhea@usm.lmu.de

Abstract

We use cosmological hydrodynamical simulations to understand the impact of stellar and AGN feedback on global galaxy properties at different redshifts and over a large range of masses and environments. We demonstrate how both stellar and AGN feedback are in combination responsible for shaping observed dynamical scaling relations of spheroidal and disk galaxies. Furthermore, we show how the interaction between dark and baryonic matter is affected by those feedback processes, and analyse the role of feedback processes in establishing the observed properties of spheroidal galaxies from $z = 2$ to present day. Finally, we present evidence for a co-evolution of the total density profiles and the central dark matter fractions in spheroidal galaxies, and demonstrate how this is influenced by the AGN feedback.

Keywords: galaxies: evolution – formation – dark matter, methods: numerical

1 Simulations and galaxy classification

The Magneticum Pathfinder[1] simulations are a set of hydrodynamical cosmological boxes of different sizes and resolutions. They include stellar feedback from SNIa and SNII, stellar winds, and AGN feedback from black holes. The metal enrichment and star formation follow the pattern of metal production from SNIa, SNII, and AGB stars, and the gas cooling depends on the local metallicity. Furthermore, several improvements for SPH were included to more accurately treat turbulence and viscosity. This results in a self-consistent formation of galaxy populations which successfully reproduce observed properties (Remus et al., 2015; Teklu et al., 2015; Remus et al., 2016). For more details on the simulations see also Hirschmann et al. (2014).

The classification of the galaxies into spheroidals and disks is based on the circularity parameter of the orbits of their stellar particles and the fraction of cold gas, as described by Teklu et al. (2015) and Remus et al. (2016). In brief, if the majority of the stellar particles have circularities close to one, the galaxy is classified as a disk. Galaxies where the majority of stellar particles have circularities close to zero are classified as spheroidals.

[1]www.magneticum.org

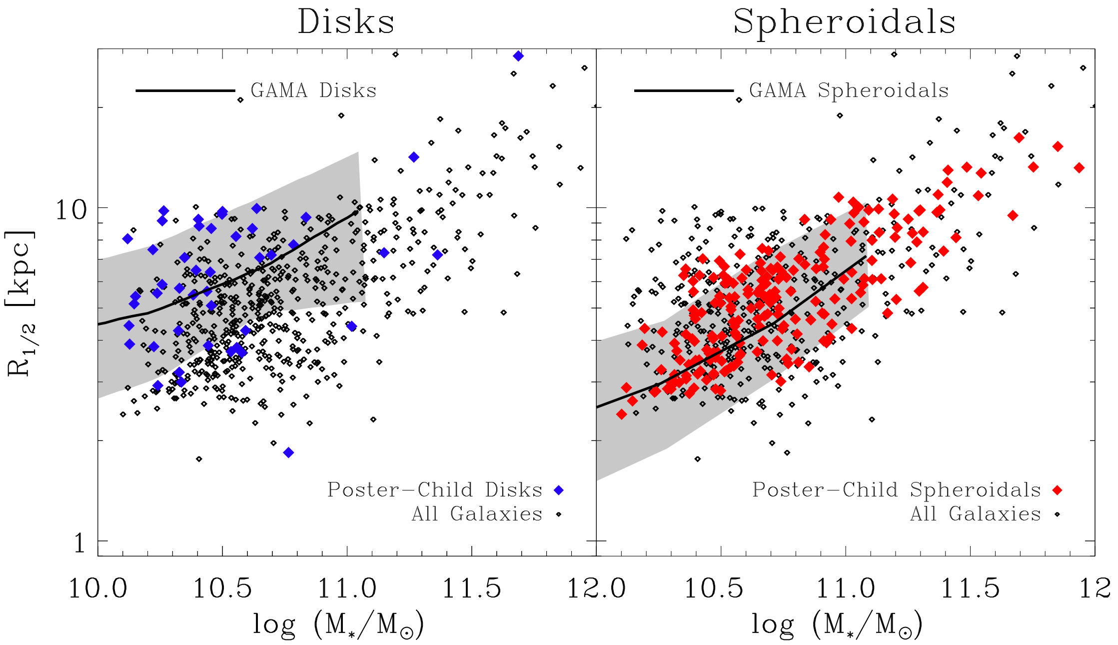

Figure 1: *Mass–size relation for Magneticum galaxies (symbols) in comparison to observations from the GAMA survey (shaded areas; Baldry et al., 2012). Left: For disk galaxies (blue symbols). Right: For spheroidal galaxies (red symbols). For reference, black symbols denote the complete sample of Magneticum galaxies in both panels. The difference in the observed mass–size relations for disks and spheroidals is well represented by the Magneticum disks and spheroidals.*

2 Scaling relations for disks and spheroidals

Observationally, it is well established that the sizes of galaxies are closely correlated with their stellar masses. However, the mass–size relations differ for disks and spheroidals: generally, at the same stellar mass, disk galaxies are larger than their spheroidal counterparts (e.g., Shen et al., 2003; Baldry et al., 2012).

The Magneticum galaxies successfully reproduce these scaling relations for both disks and spheroidals at $z = 0$, as shown in Fig. 1. This holds true also at higher redshifts, as demonstrated by Remus et al. (2016) for the Magneticum spheroidals.

Another important observed scaling relation of galaxies is the fundamental plane. It describes the relation between the size, the central velocity dispersion, and the mean central surface brightness of galaxies. For comparisons with simulations, the mass–fundamental plane is more suitable, where the stellar mass surface density is used instead of the surface brightness. Fig. 2 shows this mass–fundamental plane for the Magneticum galaxies (filled symbols), including fitting relations for observations from the SDSS survey (Hyde & Bernardi, 2009; Bezanson et al., 2015).

The Magneticum galaxies show a similar slope of the relation as the observations (this is especially true for the Magneticum spheroidals), but the relation has a slight offset of the order of the scatter of the individual galaxies. Due to the stringent criterion for classifying galaxies as disks, the chosen sample of Magneticum disks is small and may not reflect the general properties of the population.

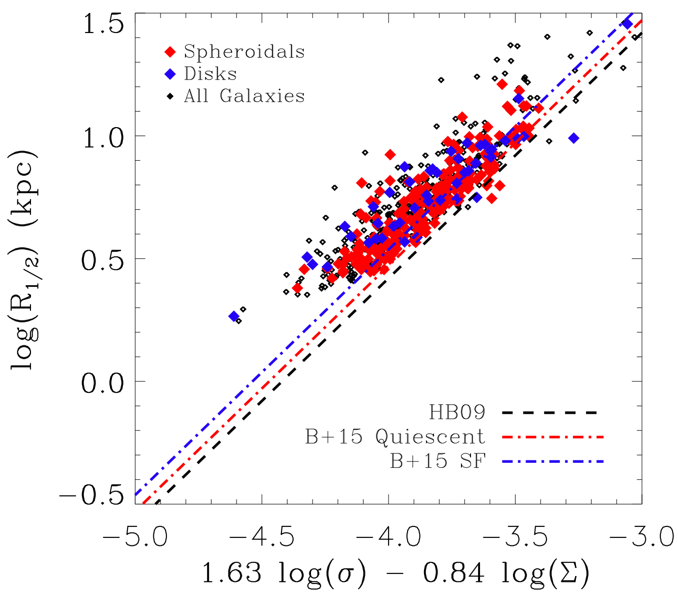

Figure 2: *Mass–fundamental plane for the Magneticum galaxies as labeled. For comparison, fits to the observations from SDSS are shown: for spheroidal galaxies (black dashed line; Hyde & Bernardi 2009), and for quiescent and star forming galaxies (red and blue dash-dotted lines; Bezanson et al. 2015).*

3 The role of AGN feedback

As shown before, a proper treatment of the feedback is important to reproduce the observed scaling relations in cosmological simulations. To understand the impact of the different feedback models on these scaling relations, we compare the Magneticum spheroidals to spheroidal galaxies from zoom-simulations without stellar winds and AGN feedback (Oser et al., 2010, 2012). A thorough investigation of these two samples of spheroidal galaxies is presented by Remus et al. (2016), where we demonstrate that the inclusion of a proper AGN feedback is already necessary at high redshifts to reproduce the observed mass–size relations, and it especially influences the fraction of quiescent galaxies at $z = 2$ (see Steinborn et al., 2015).

One particularly interesting relation that depends sensitively on the AGN feedback is the correlation between the central dark matter fractions f_{DM} and the slopes of the total (stellar plus dark matter) radial density profiles γ_{tot} (see Remus et al., 2013, 2016, for more details). This correlation is shown for both samples of spheroidals in Fig. 3 together with the observed relation from Tortora et al. (2014). Both simulations (with and without AGN feedback) show a close correlation between the two parameters. However, as this figure strikingly demonstrates, only the Magneticum sample, which includes AGN feedback and stellar winds, shows a general agreement with the observations, while the correlation found for the spheroidals without AGN feedback has a very different (much steeper) slope.

This behaviour does not depend on redshift, as the spheroidals evolve along the respective correlations. This is also indicated by Fig. 3, where filled symbols represent spheroidals at $z = 0$, while open symbols represent spheroidals at higher redshifts. Furthermore, both f_{DM} and γ_{tot} are also closely correlated with the central mass surface densities, as demonstrated by Remus et al. (2016).

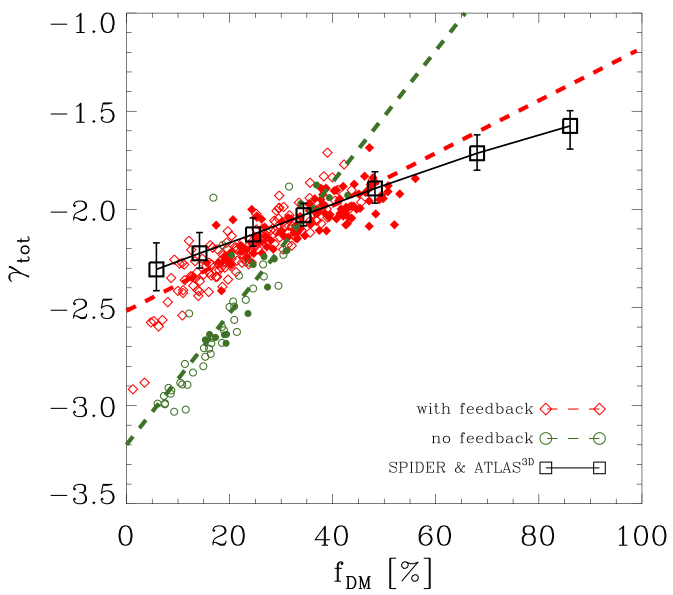

Figure 3: *Slopes of the total radial density profiles $\gamma_{\rm tot}$ versus the central dark matter fraction $f_{\rm DM}$ for Magneticum spheroidals (with AGN feedback, red diamonds) and for spheroidals without AGN feedback (green circles, Oser et al. 2010). The slope of this correlation is strongly influenced by the AGN feedback. The relation found for the Magneticum spheroidals agrees well with the observed relation found by Tortora et al. (2014) from the SPIDER and ATLAS^{3D} surveys (black line and symbols). For more details, see Remus et al. (2016).*

4 Conclusions

With the Magneticum Pathfinder simulations we can successfully reproduce galaxy scaling relations such as the mass–size relations or the mass–fundamental plane. We find an additional tight correlation between the central dark matter fractions and the total density distribution of spheroidals, established by the individual formation histories depending on the amount dry and wet accretion. The included feedback has crucial influence on all these relations, which thus can be used to test the different feedback models.

References

Baldry I. K., Driver S. P., Loveday J., et al., MNRAS **421**, 621 (2012)
Bezanson R., Franx M., & van Dokkum P. G., ApJ **799**, 148 (2015)
Hirschmann M., Dolag K., Saro A., et al., MNRAS **442**, 2304 (2014)
Hyde J. B. & Bernardi M., MNRAS **396**, 1171 (2009)
Oser L., Ostriker J. P., Naab T., et al., ApJ **725**, 2312 (2010)
Oser L., Naab T., Ostriker J. P., & Johansson P. H., ApJ **744**, 63 (2012)
Remus R.-S., Burkert A., Dolag K., et al., ApJ **766**, 71 (2013)
Remus R.-S., Dolag K., Bachmann L. K., et al., in: Ziegler B. L., Combes F., Dannerbauer H., & Verdugo M. (eds.), IAU Symposium **309**, 145 (2015)
Remus R.-S., Dolag K., Naab T., et al., ArXiv e-prints **1603.01619** (2016)
Shen S., Mo H. J., White S. D. M., et al., MNRAS **343**, 978 (2003)
Steinborn L. K., Dolag K., Hirschmann M., et al., MNRAS **448**, 1504 (2015)
Teklu A. F., Remus R.-S., Dolag K., et al., ApJ **812**, 29 (2015)
Tortora C., La Barbera F., Napolitano N. R., et al., MNRAS **445**, 115 (2014)